J. Fluid Mech. (1969), *vol.* 36, *part* 3, *pp.* 485–503
Printed in Great Britain

The turbulent boundary layer in a corner

By G. M. BRAGG†
Engineering Department, University of Cambridge

(Received 10 February 1968 and in revised form 15 October 1968)

Turbulent flow along the axis of a 90° corner is considered. Experimental measurements of velocities, wall shear stresses and $\overline{u'^2}$, the turbulent normal stress in the streamwise direction, have been made. The data are considered both from the point of view of momentum integral and similarity analyses. A suitable momentum integral equation is easily derived but difficult to use due to the form of the terms which must be measured. Similarity techniques give a series of correlations which describe the flow over a narrow range of Reynolds number for which data are available. There is experimental evidence for secondary currents in this type of flow but their analysis presents considerable difficulty.

1. Introduction

The turbulent boundary layer in a corner represents a fairly simple three-dimensional turbulent flow and has some practical importance. We may expect that the problem will be complicated by the presence of secondary flows of the type found in fully developed flow in non-circular ducts. Previous work on flows of this sort has been done by Eichelbrenner (1961, 1965), Gersten & Miyashiro (1960) and others. The findings of Paradis (1963) are also relevant. Early work was mainly concerned with analyses of the '1/7 power law' type extended to the corner region.

As is usual in turbulent shear flows exact analytical techniques are impossible. However, by making assumptions of the kind that are commonly used in turbulent boundary-layer theory we may arrive at simplified forms of the Navier–Stokes equations, including Reynolds stresses. The assumptions made are: (i) that rates of variation of quantities in the streamwise direction are small with respect to changes of the same quantities in the direction orthogonal to the free stream flow and, (ii) that turbulent fluctuations are small with respect to the main streamwise velocities. On this basis we may arrive by the usual methods at simplified forms of these equations. It should be noted that within the region considered the equations might locally assume even simpler forms. For example, near one wall far from the corner the equations will take the form usual to two-dimensional turbulent boundary layers.

Assume a Cartesian system as in figure 1 with axes x, y and z and velocity components, U, V and W respectively. The x-axis lies along the axis of the corner

† Present address: Department of Mechanical Engineering, University of Waterloo, Waterloo, Ontario.

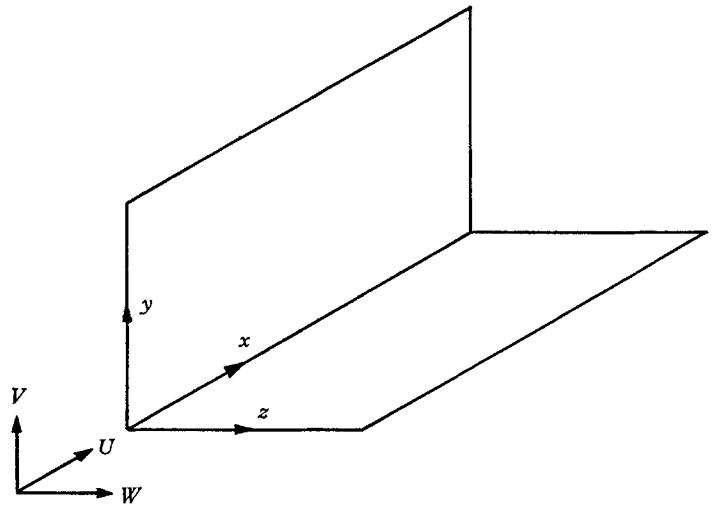

FIGURE 1. Reference system.

with the origin at the leading edge of the two walls and the y- and z-axes oriented along the leading edges of the walls which are at 90° to each other.

If we retain only terms of first-order (i.e. rejecting terms of order δ and δ^2 in the usual terminology by assuming that the secondary velocities are of the order of V_∞, the normal velocity at the edge of the boundary layer) we arrive at:

$$U\frac{\partial U}{\partial x}+V\frac{\partial U}{\partial y}+W\frac{\partial U}{\partial z}=-\frac{1}{\rho}\frac{dP}{dx}+\frac{1}{\rho}\frac{\delta\tau_{xy}}{\partial y}+\frac{1}{\rho}\frac{\partial\tau_{xz}}{\partial z} \tag{1}$$

and

$$\frac{\partial U}{\partial x}+\frac{\partial V}{\partial y}+\frac{\partial W}{\partial z}=0, \tag{2}$$

where

$$\tau_{xy}=\rho\left(\nu\frac{\partial U}{\partial y}-\overline{u'v'}\right)$$

and

$$\tau_{xz}=\rho\left(\nu\frac{\partial U}{\partial z}-\overline{u'w'}\right).$$

The y- and z-direction equations contain no first-order terms.

It is obvious that if any details of the flow such as possible secondary currents are to be accurately described we must use equations containing more terms than equations (1) and (2) but we hope that these equations might serve as a useful description of the overall flow in that corner region. As mentioned before, the equations could be simplified if local regions within the corner flow were considered.

2. Experiments

The experimental arrangement consisted of two plates 16 in. wide by 56 in. long by $\frac{5}{8}$ in. thick arranged at right angles to each other and sealed along the vertex. The leading edges were faired and trip wires 0·024 in. in diameter were

placed 1 in. from the leading edges. The plates were mounted symmetrically in a wind tunnel. To obtain an adverse pressure gradient in the boundary layer, blocking plates were arranged 37 in. downstream from the trip wire and the height adjusted locally so that the pressure distributions were as nearly as possible the same at different distances from the corner. Static pressure holes were tapped at a series of points on both surfaces. The pressure distributions for the two cases studied are shown in figure 2. Henceforth in this paper the experiments performed under nearly zero pressure gradient will be called series I and those performed under the adverse pressure gradient conditions will be called series II.

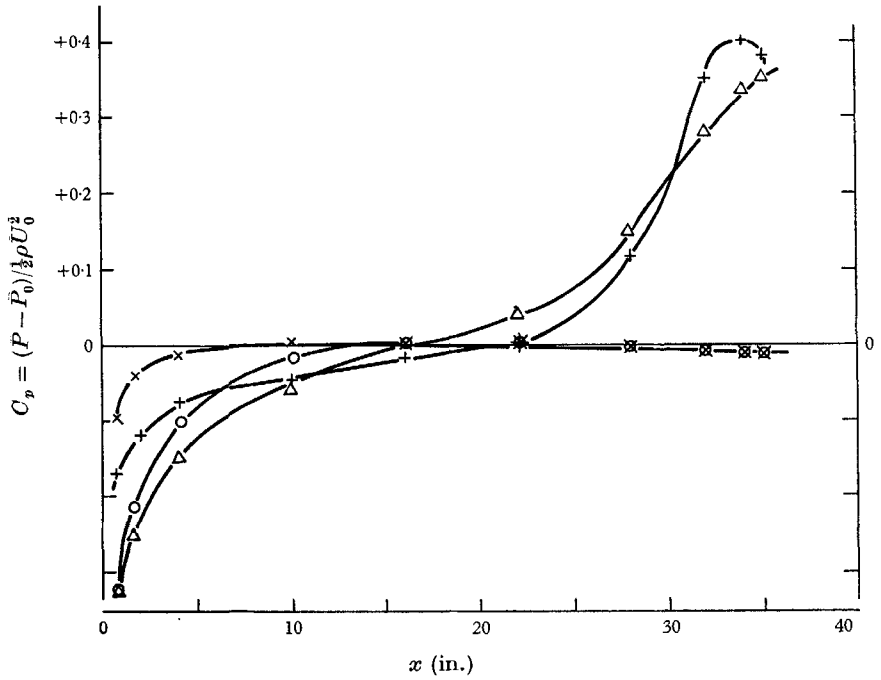

FIGURE 2. Static pressure distributions at 1 in. from the vertex and 12 in. from the vertex for the two pressure gradients measured. Series I: ○, $Y = Z = 1$ in.; ×, $Y = Z = 12$ in. Series II: Δ, $Y = Z = 1$ in.; +, $Y = Z = 12$ in.

Since the plates were not of infinite width in the y- and z-directions the possibility of effects due to this fact was checked. The plates were widened by 8 in. and no measureable effects on wall shear stress or velocity were found in the corner region. This is not unexpected since in the worst case the width of the plates was approximatly 25 times the two-dimensional boundary-layer thickness. This is consistent with the findings of Davies & Young (1963) who found that edge effects of this sort extended only to about twice the boundary-layer thickness from the edge.

The velocities were measured with the aid of a Pitot tube, the turbulent fluctuations using a commercial hot-wire anemometer and the wall shear stresses were evaluated by the Preston tube method. In each case where a wall shear

stress is presented at least two data points on a line normal to the surface were checked against the standard 'inner law' relationships.

It was found that very near each wall the 'inner law' relationships gave an accurate description of the flow except very close to the corner.

Considerable difficulties were encountered in obtaining a flow which was closely symmetrical about the bisecting plane of the corner. Any small difference in upstream conditions between the two plates caused considerable asymmetry of the flow. This problem has also been encountered by Gessner & Jones (1961) and by Paradis (1963). The implication of this is that a closely symmetrical flow is unlikely to occur in other than closely controlled laboratory conditions.

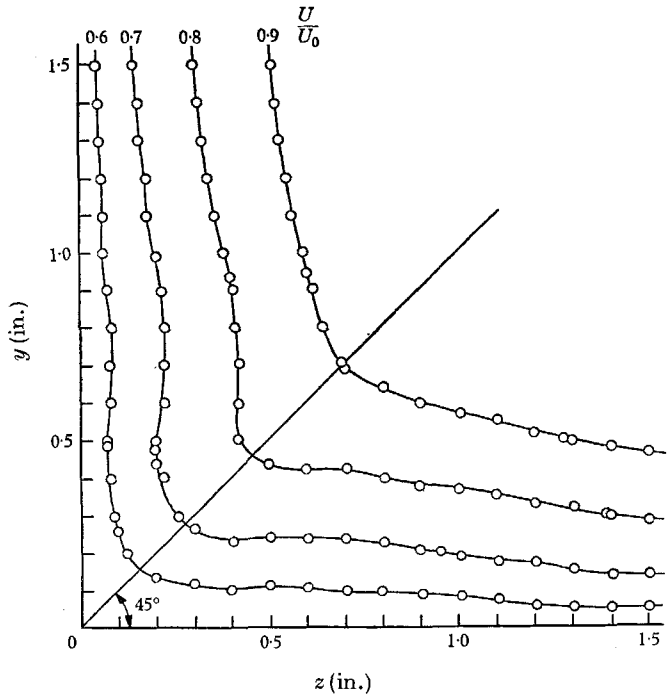

FIGURE 3. Isotach plot of velocities in the corner, $X = 30$ in. $U_0 = 75{\cdot}6$ ft./sec, $R_{\theta_2} = 3370$. Series I.

Typical plots of mean flow velocities, $\sqrt{u'^2}$, and wall shear stresses are presented in figures 3–5 for zero pressure gradient. The Reynolds number is 3370 using free-stream velocity and the boundary-layer momentum thickness at the same streamwise position but far from the corner. Additional measurements of velocities, $\sqrt{u'^2}$ and wall shear stresses were made at $R_{\theta_2} = 2740$ and 3060 in the zero pressure gradient flow and $R_{\theta_2} = 2510$, 3140 and 3960 in the adverse pressure gradient flow. This data showed similar behaviour to that presented here. Reliable measurements of secondary currents have yet to be made but it is expected that the technique of Brundrett & Baines (1964) should furnish quite reliable data. More complete descriptions and tabulations of the measurements may be found in Bragg (1965).

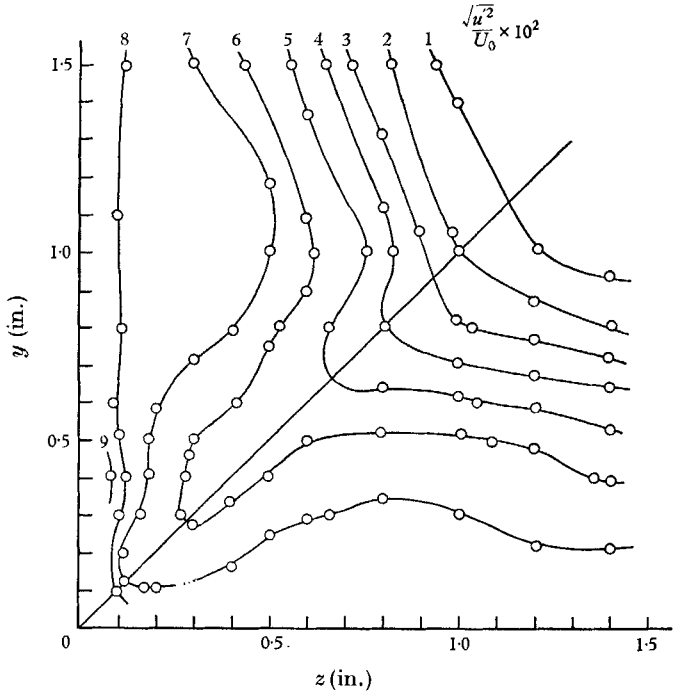

FIGURE 4. Lines of constant $\sqrt{u'^2}/U_0$, series I, $X = 30$ in, $R_{\theta_2} = 3370$.

3. Momentum integrals

A useful form of (1) and (2) may be derived by integrating (1) over y and z and eliminating the velocities V and W by the use of (2). This will give an integral relation very similar to the momentum integral equation used in the study of two-dimensional boundary layers. It is possible to integrate a set of equations containing second-order terms with respect to y and z, but the resulting relation includes triple integrals and is therefore not practically useful.

If we perform the integration of (1) and make use of the symmetry of the flow we can obtain

$$\frac{\partial}{\partial x}\int_0^h\int_0^h (U_0 U - U^2)\,dy\,dz + \frac{dU_0}{dx}\int_0^h\int_0^h (U_0 - U)\,dy\,dz = 2\int_0^h \frac{\tau_0(z)}{\rho}\,dz, \qquad (3)$$

where h is very much greater than the range of y and z under consideration, U_0 is the free stream velocity and $\tau_0(z)$ is the wall shear stress on the $y = 0$ wall. A necessary assumption in deriving this equation is that

$$2\int_0^h dz\,[V(U_0 - U)]_{y=h}$$

is zero. This does not contradict continuity if we assume that $V = 0$ only in the region where $U_0 - U \neq 0$ and that this region is small with respect to h. An equation similar to (3) has been derived by Louis (1958) and Gersten & Miyashiro (1960) also derive a similar equation. The advantage of Gersten & Miyashiro's

(1960) equation is that by subtracting an 'equivalent two-dimensional form' from (3) they obtain integral quantities which tend to a finite limit as $h \to \infty$. The disadvantage of this form is that the values of the integrated quantities turn out to be extremely small when evaluated experimentally and therefore have margins of error several times larger than the evaluated quantity, i.e. the effect of the corner on integrated quantities other than wall shear stress is less than errors of measurement. It seems then that (3) represents the most useful form at present if momentum integral techniques are to be used to describe corner flow. The data from the present experiments were used to evaluate both sides of (3) and the discrepancy was of the order of 10 % in the worst case. This is similar to the experimental agreement obtained in similar checks with the two-dimensional momentum integral equation. The agreement was worst near separation in the adverse pressure gradient case as might be expected and was closer to 5 % in the worst case of the zero pressure gradient data.

4. The viscous corner region

Deep in the corner region we may expect that the turbulent fluctuations are small. For zero pressure gradient we assume that, as in the analogous two-dimensional case very near the wall, the flow is described by the laminar solutions.

The laminar case has been studied by Pearson (1957) who assumed a solution of the form

$$U/U_0 = A_1 + A_2\eta\zeta + A_3\eta^2\zeta^2 + A_4\eta^3\zeta^3 + \ldots, \tag{4}$$

where A_1 must be zero and

$$\eta = y\sqrt{(U_0/\nu x)} \quad \text{and} \quad \zeta = z\sqrt{(U_0/\nu x)}.$$

Very close to the wall we may consider only the first non-zero term in (4) and then

$$U/U_0 = A_2\eta\zeta$$

or

$$U/U_0 = A_2 U_0 yz/\nu x. \tag{5}$$

We define a velocity scale U_c, where

$$U_c = \left(\nu^2 \frac{\partial^2 U}{\partial y\,\partial z}\bigg|_{\substack{y=0\\z=0}}\right)^{\frac{1}{3}}.$$

Substitution of this in (5) gives

$$U/U_c = (U_c y/\nu)\,(U_c z/\nu). \tag{6}$$

This is a form closely analogous to the form

$$U/U_\tau = U_\tau y/\nu$$

used to describe the form of the velocity profile close to the wall in the two-dimensional turbulent boundary layer.

It is interesting to note from (6) that at the corner the gradient of velocity along the bisecting plane is zero. This is required if discontinuities in fluid stresses are to be avoided in the region.

Unfortunately it was not possible in the present experiments to test (6) against experimental data since it was not possible to measure velocities sufficiently close to the corner.

5. Wall shear stresses

The general behaviour of the wall shear stresses may be seen in figures 5 and 6. In general terms, as the corner is approached the wall shear drops slowly over the outer part of the corner region to a value of approximately $0{\cdot}75\tau_{02}$ where τ_{02} is

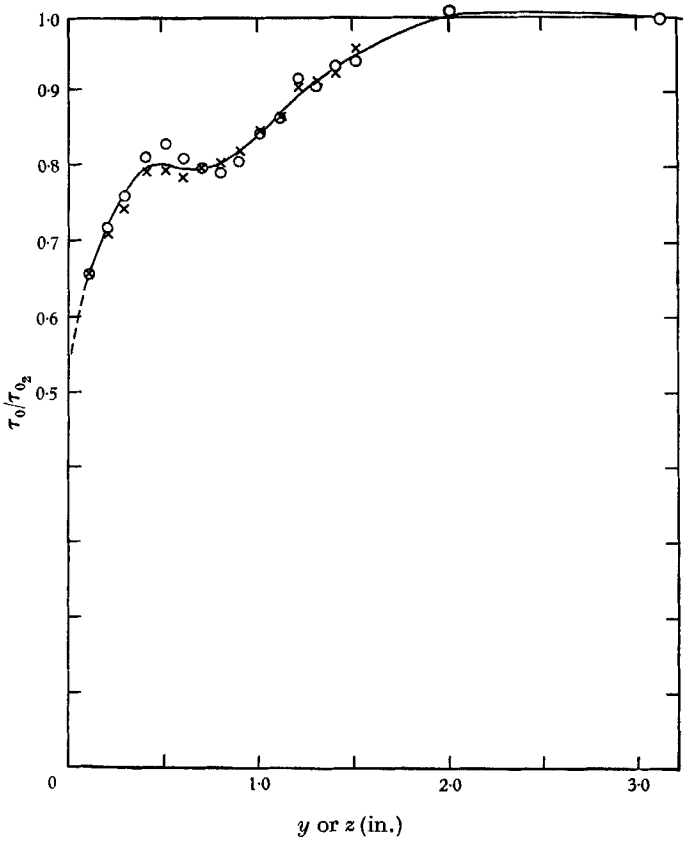

FIGURE 5. Wall shear stresses in zero pressure gradient: ×, $Y = 0$; ○, $Z = 0$; series I, $X = 30$ in., $R_{\theta_2} = 3370$, $\tau_{0_2} = 0{\cdot}0195$ lb./ft.^{2} at $Y = 5{\cdot}3$ in.

the value very far from the corner. At this point there is an inflexion, where the shear stress seems to rise again or at least stay constant for a small distance. Closer to the corner the wall shear stresses will drop to zero since at $y = 0$, $\partial u/\partial z = 0$.

It is natural to introduce U_{τ_2}, where U_{τ_2} is the wall shear velocity far from the corner, as a velocity scale which may describe part of the wall shear stress distribution. Values of $U_\tau = \sqrt{(\tau_0/\rho)}$ are plotted in figure 7 as values of U_τ/U_{τ_2} *versus*

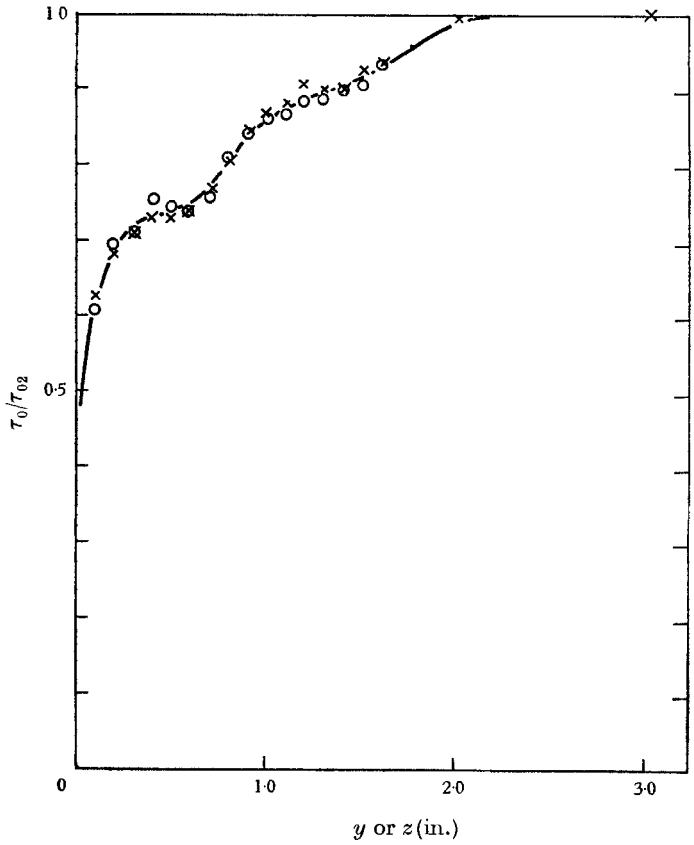

FIGURE 6. Wall shear stresses in adverse pressure gradient: ○, $Y = 0$; ×, $Z = 0$, series II, $X = 20$ in., $R_{\theta_2} = 2510$, $\tau_{02} = 0{\cdot}0198$ lb/ft.^{2} at $Y = 5{\cdot}3$ in.

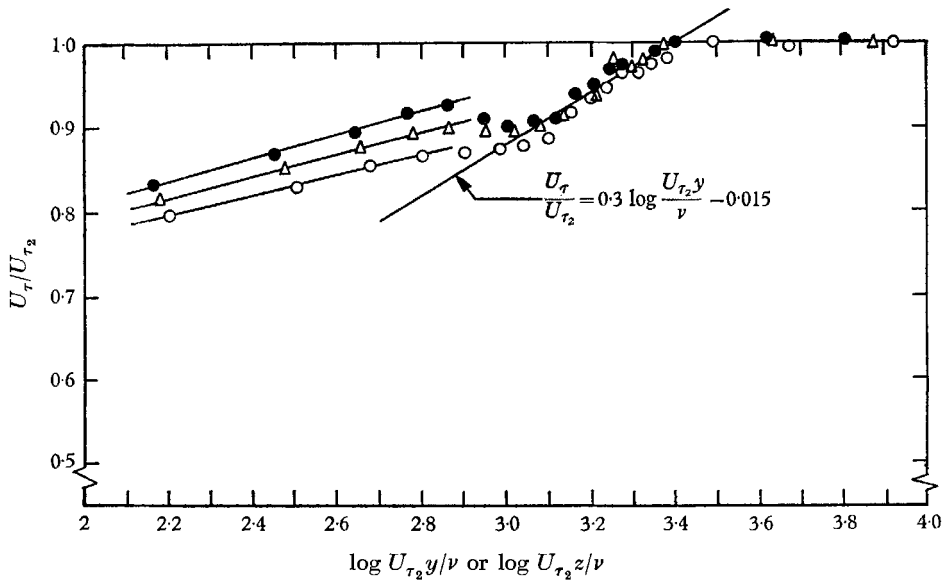

FIGURE 7. Wall shear stresses in the corner in zero pressure gradient. Series I: ○, $R_{\theta_2} = 2740$; △, $R_{\theta_2} = 3060$; ●, $R_{\theta_2} = 3370$. Average values for the two walls are given.

$\log(U_{\tau_2}y/\nu)$ or $\log(U_{\tau_2}z/\nu)$. It is seen that this type of plot gives an empirical correlation over the range

$$1000 < U_{\tau_2}y/\nu < 2520,$$

for the range of Reynolds numbers considered. While there is no evident reason why it should be so, it seems that the behaviour of the wall shear stress in this region may be approximated for the range of Reynolds numbers available by a straight line given by

$$U_\tau/U_{\tau_2} = 0{\cdot}3\log(U_{\tau_2}y/\nu) - 0{\cdot}015.$$

This region takes in approximately 60 % of the region of corner influence. In addition we see that $U_{\tau_2}y/\nu = 2520$ may be used as an empirical measure of the region of influence of the corner on the wall shear stress. At the experimental range of Reynolds numbers this corresponds to a value of approximately 2δ, where δ is the thickness of the boundary layer far from the corner. It is easily seen that even the postulated empirical relationship does not correlate the wall shear stress closer to the corner than $U_{\tau_2}y/\nu = 1000$. The difficulty obviously lies in assuming that U_{τ_2} is a velocity scale which defines the wall shear stress deep in the corner. It seems, then, that if another velocity scale was defined for this region we might be able to show some form of local similarity in this region.

A possible velocity scale for this inner region would be

$$U_c = \left(\nu \frac{\partial^2 U}{\partial y\,\partial z}\bigg|_{\substack{y=0\\z=0}}\right)^{\frac{1}{3}},$$

which is the velocity scale proposed to describe the viscous corner region. However, as stated previously it was not possible to measure this quantity in the present experiments. For practical reasons, then, it is necessary to find another velocity scale. The scale chosen will, we hope, bear a constant relationship to U_c, independent of Reynolds number. A velocity scale may be arrived at by considering the range $2{\cdot}10 \leqslant \log(U_{\tau_2}y/\nu) \leqslant 2{\cdot}85$ in figure 7 which gives the data for zero pressure gradient. We see that straight lines may be drawn through the various sets of data as shown. This implies that we may write

$$U_\tau/U_{\tau_2} = K_1\log(U_{\tau_2}y/\nu) + K_2 \tag{7}$$

for this region, where K_1 and K_2 are parameters depending on the Reynolds number and we consider for the present only zero pressure gradient.

Differentiation of (7) with respect to y and rearrangement gives

$$(y/2{\cdot}303)\,\partial U_\tau/\partial y = U_{\tau_2}K_1 = U_K,$$

where U_K is defined by this equation. U_K is seen to have the dimensions of velocity and to be a constant for each profile in the region under consideration. This quantity will be a function of Reynolds number and is easily evaluated as $U_{\tau_2}K_1$ where K_1 is the slope of the wall shear stress distribution over the region in the form U_τ/U_{τ_2} *vs.* $\log(U_{\tau_2}y/\nu)$.

Now since $U_K = U_{\tau_2}K_1$ we may substitute for U_{τ_2} in (7). Then

$$U_\tau/U_K = \log(U_K y/\nu) + F, \tag{8}$$

where $F = (K_2/K_1) - \log K_1$. F must, until proven otherwise, be assumed a function of Reynolds number. Values of U_τ/U_K *vs.* $\log(U_K y/\nu)$ are shown in figure 8 for the Reynolds number and pressure gradients measured. The conclusions to be drawn from this figure are that F may be considered nearly independent of Reynolds number for the range of Reynolds numbers measured and that (8) may be considered as an empirical similarity relationship predicting the wall

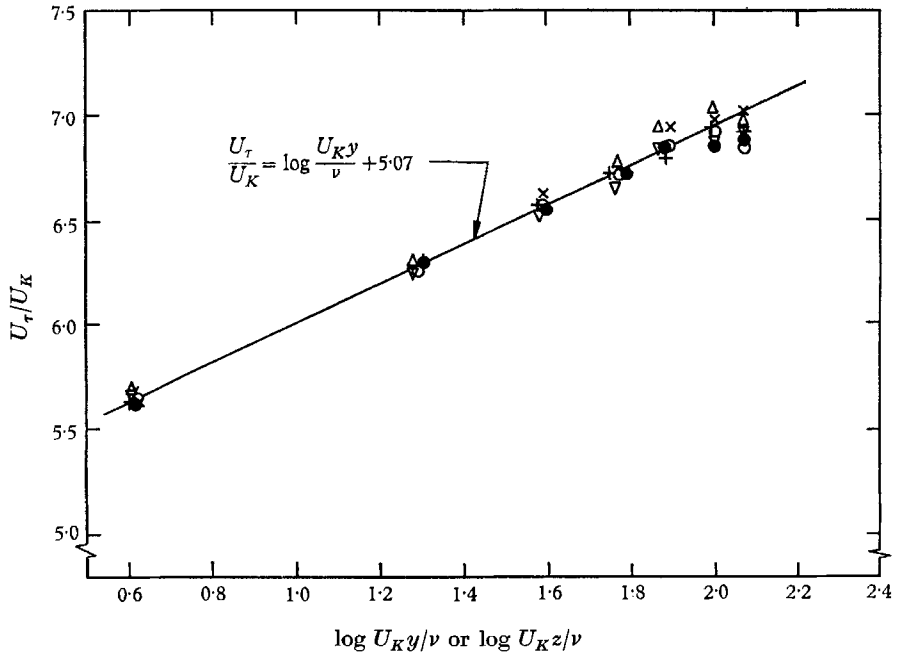

FIGURE 8. Wall shear stresses in the inner region, series I. ○, $R_{\theta_2} = 2740$, $Y = 0$; ×, $R_{\theta_2} = 2740$, $Z = 0$; ●, $R_{\theta_2} = 3060$, $Y = 0$; +, $R_{\theta 2} = 3060$, $Z = 0$; △, $R_{\theta 2} = 3370$, $Y = 0$; ▽, $R_{\theta_2} = 3370$, $Z = 0$.

shear stress distribution in the corner region for zero gradient. The value of F agreeing most closely with the data is 5·07. The collapse of data for the adverse pressure gradient case studied was poor except at a far upstream point before the pressure gradient had risen significantly. A similar form for (8) might have been arrived at by assuming a form of local similarity for this region such that U_τ was a function of U_K, y and ν only. The logarithmic form of (8) is implicit in our definition of the velocity scale U_K but it is still necessary to revert to experiments to show that F is nearly independent of Reynolds number and therefore that U_τ is a function of U_K, y and ν only. It should be noted that experimental evidence justifies this relation only down to $\log(U_K y/\nu) = 0{\cdot}6$. It should also be noted that the 'log law' of two-dimensional turbulent boundary layers may be arrived at by reasoning similar to that used in deriving (8).

6. Mean streamwise velocities

The experiments undertaken showed that near each wall quite far into the corner, the two-dimensional inner law correlated the mean flow velocities quite well. As far into the corner as it was possible to measure velocities and wall shear stresses, the inner law describes the flow out to a value of $U_\tau y/\nu$ of approximately 60 if U_τ is the wall shear stress on the $y = 0$ wall and y is the distance normal to the wall. Far from the corner the region described by the inner law will be the same as in the two-dimensional boundary layer. This decrease in the range of y for which the logarithmic law is valid is obviously due to the influence of the $z = 0$ wall. The fact that the inner law describes the flow when $y \gg z$ or when $z \gg y$ is the justification for the use of Preston tubes to measure wall shear stresses. This behaviour is similar to that found by Leutheusser (1963) in fully developed flow in square ducts.

There is a region deep in the corner and near the plane of symmetry but still in the fully turbulent region where the velocity gradients are large but where the velocities are not correlated by the usual logarithmic law. This region is likely to exhibit local similarity although here the effect of both walls will need to be taken into account.

If local similarity does apply in this region is should be possible to describe U as a function of the wall shear stresses: the lengths y and z and the fluid properties μ and ρ. Then

$$U = f_1(U_{\tau_y}, U_{\tau_z}, \nu, y, z),$$

where U_{τ_y} and U_{τ_z} are defined as the wall shear velocities on the $y = 0$ and $z = 0$ walls respectively. However our consideration of the wall shear stresses led to the conclusion that for the turbulent inner region of the corner

$$U_{\tau_y} = f_2(U_K, z, \nu)$$

and

$$U_{\tau_z} = f_2(U_K, y, \nu).$$

We may then write

$$U = f_3(U_K, \nu, y, z)$$

without loss of generality. In non-dimensional form this becomes

$$U/U_K = f_4(U_K y/\nu, U_K z/\nu). \tag{9}$$

This relation will hold if the flow in the region considered is completely determined by local wall shear stresses, the fluids properties and the distance from each wall.

Consider now the outer region of the corner boundary layer. We confine ourselves for the present to the case of zero streamwise pressure gradient. In the two-dimensional case the flow in this region is described by the velocity defect law

$$(U_0 - U)/U_\tau = g_1(y/\delta_2) \tag{10}$$

where $y = \delta_2$ defines the edge of the boundary layer.

In general terms this law is derived by reasoning that the velocity defect in the outer region is independent of viscosity and is a function of the wall shear

stress and the distance from the wall, δ_2, to which the effect has diffused. By this argument

$$U_0 - U = g_2(y, \delta_2, u_\tau)$$

from which (10) follows.

The arguments leading in the two-dimensional case to the velocity defect law suggest for the corner flow the relation

$$U_0 - U = g_3(y, z, U_K, \delta'). \tag{11}$$

δ' is defined as the distance measured along the plane of symmetry from the corner to where

$$U/U_0 = 0{\cdot}99.$$

U_K is the velocity scale determining the shear stress deep in the corner. Strictly speaking, $U_0 - U$ should also be dependent upon U_{τ_2}. If we restrict our argument to the flow adjacent to the region of wall shear stresses described by (8) and near the plane of symmetry, the influence of U_K should be large compared to the influence of U_{τ_2} and (11) should be a valid approximation. Writing (11) in dimensionless form we obtain

$$(U_0 - U)/U_K = g_4(y/\delta', z/\delta'). \tag{12}$$

We now enquire, as in an analogous derivation of the two-dimensional logarithmic law, whether or not there is a region over which both (9) and (12) are valid. If there is a region of overlap the functional form which f_4 and g_4 may take is restricted. We may write (9) as

$$U/U_K = f_4[(y/\delta')(U_K\delta'/\nu), (z/\delta')(U_K\delta'/\nu)] \tag{13}$$

and (12) as

$$U/U_K = (U_0/U_K) - g_4(y/\delta', z/\delta'). \tag{14}$$

These are two expressions for the same quantity if the two regions overlap. In (13) the factors y/δ' and z/δ' are multiplicative factors and in (14) are additive. The functions f_4 and g_4 must therefore take a logarithmic form. There are, of course, an infinite number of forms which fit this requirement. The simplest form, however, has been found suitable in the analogous two-dimensional case. A simple form which (9) and (12) may take is

$$U/U_K = G\log(U_K y/\nu) + G\log(U_K z/\nu) + H \tag{15}$$

and

$$(U_0 - U)/U_K = -G\log(y/\delta') - G\log(z/\delta') + I. \tag{16}$$

Far from the corner, but inside the boundary layer and near the plane of symmetry, we may expect that the more general form

$$(U_0 - U)/U_K = g_4(y/\delta', z/\delta')$$

will still be retained. Equations (15) and (16) may, of course, be written in the form

$$U/U_K = G\log(U_K^2 yz/\nu^2) + H$$

and

$$(U_0 - U)/U_K = -G\log(y^2/\delta'^2) + I.$$

Along the plane of symmetry these equations take the form

$$U/U_K = 2G\log(U_K y/\nu) + H \tag{17}$$

and

$$(U_0 - U)/U_K = -2G\log(y/\delta') + I. \tag{18}$$

It is, of course, possible to replace y by z in (17) and (18) due to the symmetry of the flow.

If these equations hold over a region, a unique relationship exists between U_0, δ' and U_K, since U, y, and z may be eliminated by addition of (15) and (16). We then obtain

$$U_0/U_K = G\log(U_K^2\delta'^2/\nu^2)+H+I$$

or

$$U_0/U_K = G\log R_{\delta'}^2(U_K/U_0)^2+H+I, \tag{19}$$

where

$$R_{\delta'} = U_0\delta'/\nu.$$

It is now necessary to test the suggested equations against experimental results. Figure 9 gives values of U/U_K plotted against $\log(U_K y/\nu)$ along the plane of

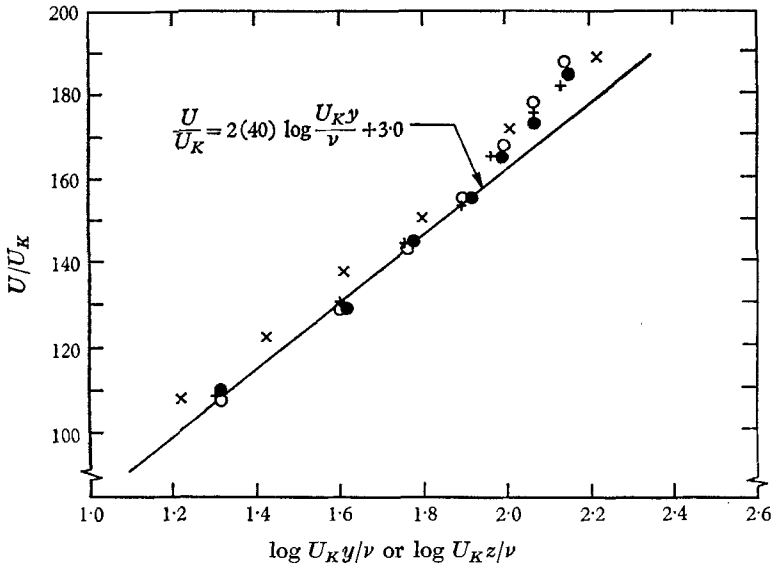

FIGURE 9. Velocities along the plane of symmetry, inner region, series I and after Paradis (1963). ○, $R_{\theta_2} = 2740$; ●, $R_{\theta_2} = 3060$; +, $R_{\theta_2} = 3370$; ×, $R_{\theta_2} = 19400$, Paradis (1963).

symmetry for the zero pressure gradient flow and figure 10 gives the same data for the case of adverse pressure gradient. The velocities are indeed seen to fall, within the range of accuracy of the data, along a straight line for zero pressure gradient for $\log(U_K y/\nu) < 1{\cdot}95$. This line is given by

$$U/U_K = 2(40)\log(U_K y/\nu)+3{\cdot}0.$$

The correlation fails in the adverse pressure gradient for $R_{\theta_2} = 3960$ but shows fairly good agreement for $R_{\theta_2} = 2510$ and 3140 out to $\log(U_K y/\nu) \approx 1{\cdot}9$. In figures 11 and 12, $(U_0 - U)/U_K$ is plotted against $\log(y/\delta')$ for the two pressure gradients. The correlation is excellent for the zero pressure gradient and for $R_{\theta_2} = 2510$ in the adverse pressure gradient, but is only fair for $R_{\theta_2} = 3140$ and poor for $R_{\theta_2} = 3960$ in the adverse pressure gradient. The outer flow not

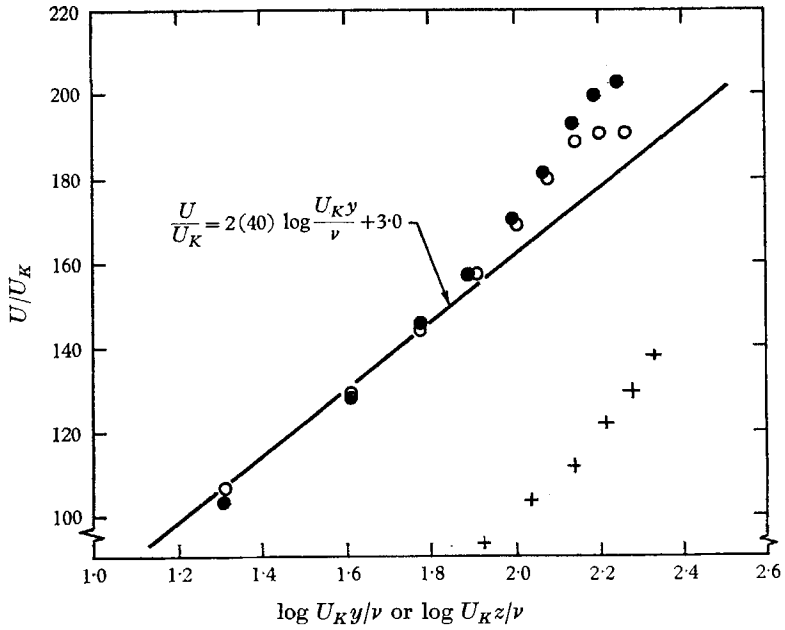

FIGURE 10. Velocities along the plane of symmetry, inner region, series II. ○, $R_{\theta_2} = 2510$; ●, $R_{\theta_2} = 3140$; +, $R_{\theta_2} = 3960$.

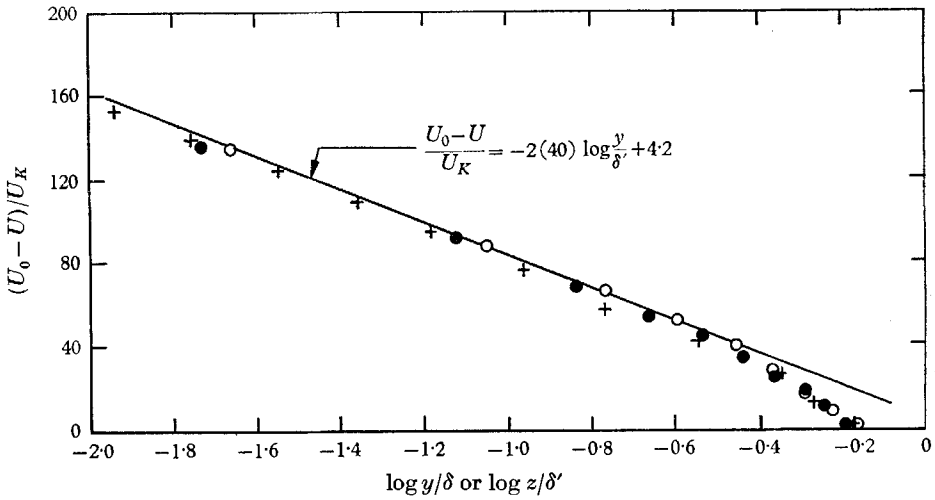

FIGURE 11. Velocities in the outer region along the plane of symmetry ○, $R_{\theta_2} = 2740$, series I. ●, $R_{\theta_2} = 3370$, series I; +, $R_{\theta_2} = 19400$, after Paradis (1963).

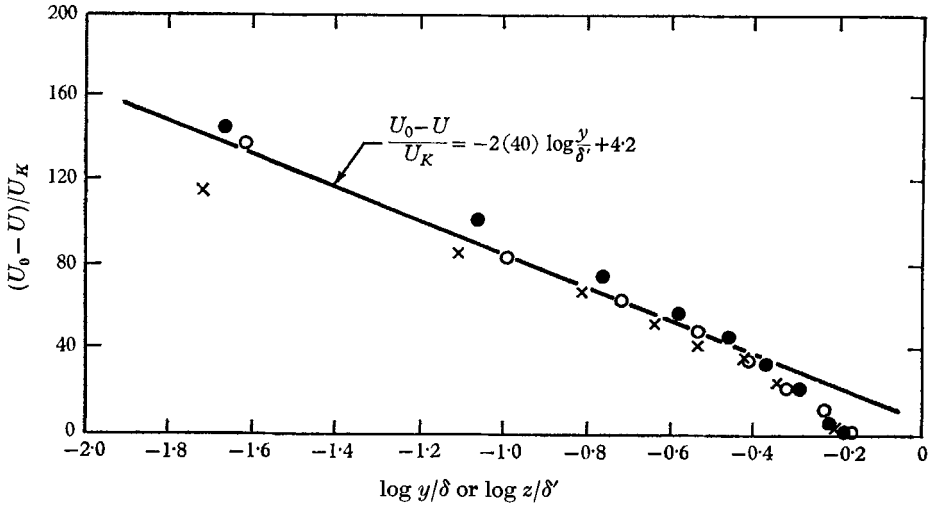

FIGURE 12. Velocities in the outer region along the plane of symmetry, series II. ○, $R_{\theta_2} = 2570$; ●, $R_{\theta_2} = 3140$; ×, $R_{\theta_2} = 3960$.

correlated by (19) is seen to fall on a unique curve for zero pressure gradient as predicted by (12).† The constants evaluated from figures 9 to 12 are

$$G = 40,$$

$$H = 3{\cdot}0,$$

$$I = 4{\cdot}2.$$

Paradis (1963) has obtained mean flow measurements for a corner boundary layer in zero pressure gradient. These results do not include detailed tabulations of velocities nor do they include measurements of wall shear stresses. For this reason, it is not possible to calculate U_K directly. Detailed data are, however, given along the plane of symmetry. It is possible to test for an increased range of applicability of the various assumptions using this data by calculating U_K from (19) using the constants obtained from the present results. The value of U_K obtained from this calculation is 0·410 feet per second. We may now plot Paradis' results as a check on the various equations. This has been done in figures 9–11. The agreement is seen to be fairly good although slightly different values for the constants would be more appropriate. The calculation of U_K by (19) is particularly sensitive to the choice of G and this would account for the slight discrepancies.

Away from the plane of symmetry but not in the region correlated by the two-dimensional logarithmic law we may also compare the measured values with those predicted by (15).

It should be noted that (15) implies that lines of U/U_K = constant, are hyperbolae of the form

$$yz = \text{constant}.$$

† Note that $U/U_0 = 0{\cdot}99$ at $y = \delta'/\sqrt{2}$ since y is measured at 45° to δ'.

The comparison with the experimental data deep in the corner is made in figures 13, 14 and 15. The agreement is fair over a range of approximately

$$10 < U_K y/\nu \quad \text{or} \quad U_K z/\nu < 60$$

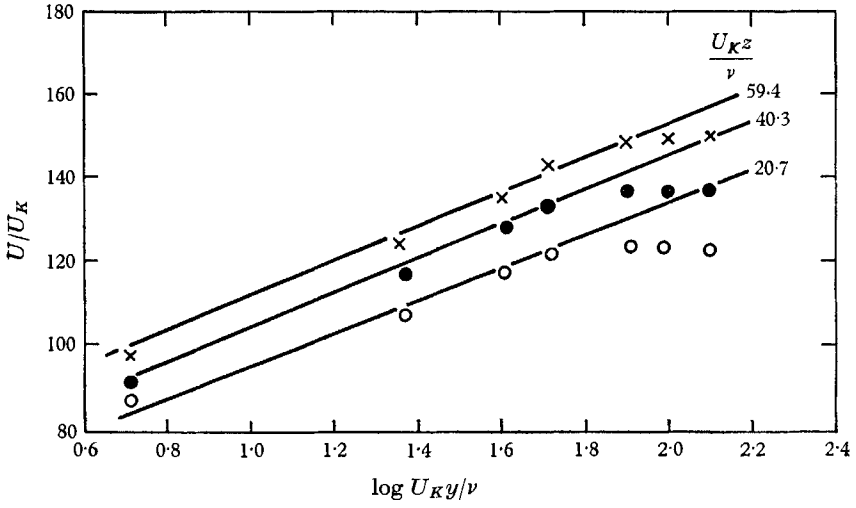

FIGURE 13. Velocities in the inner region, series I, $R_{\theta_2} = 2740$. ○, $U_K z/\nu = 20{\cdot}7$; ●, $U_K z/\nu = 40{\cdot}3$; ×, $U_K z/\nu = 59{\cdot}4$. ——, from $U/U_K = 40\log(U_K^2 yz/\nu^2) + 3{\cdot}0$.

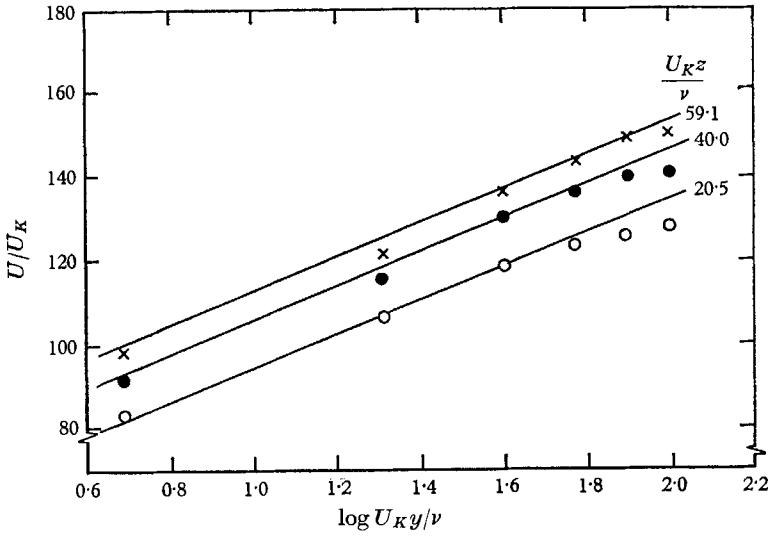

FIGURE 14. Velocities in the inner region, series I, $R_{\theta_2} = 3370$. ○, $U_K z/\nu = 20{\cdot}5$; ●, $U_K z/\nu = 40{\cdot}0$; ×, $U_K z/\nu = 59{\cdot}1$. ——, from $U/U_K = 40\log(U_K^2 yz/\nu^2) + 3{\cdot}0$.

for the zero pressure gradient cases. For the adverse pressure gradient with $R_{\theta_2} = 2510$ the agreement is rather worse. The data are not shown for the other two measured Reynolds numbers in the adverse pressure gradient but the

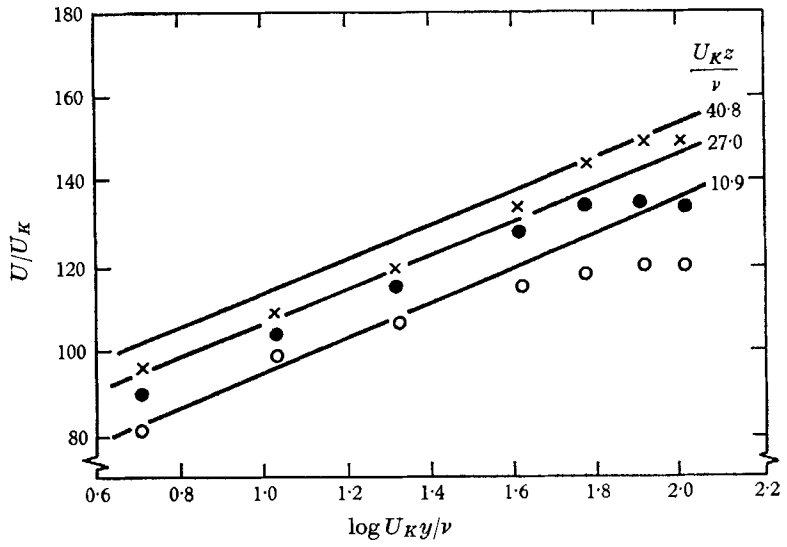

FIGURE 15. Velocities in the inner region, series II, $R_{\theta_2} = 2510$. ○, $U_K z/\nu = 10{\cdot}9$; ●, $U_K z/\nu = 27{\cdot}0$; ×, $U_K z/\nu = 40{\cdot}8$. ——, $U/U_K = 40\log(U_K^2 yz/\nu^2) + 3{\cdot}0$.

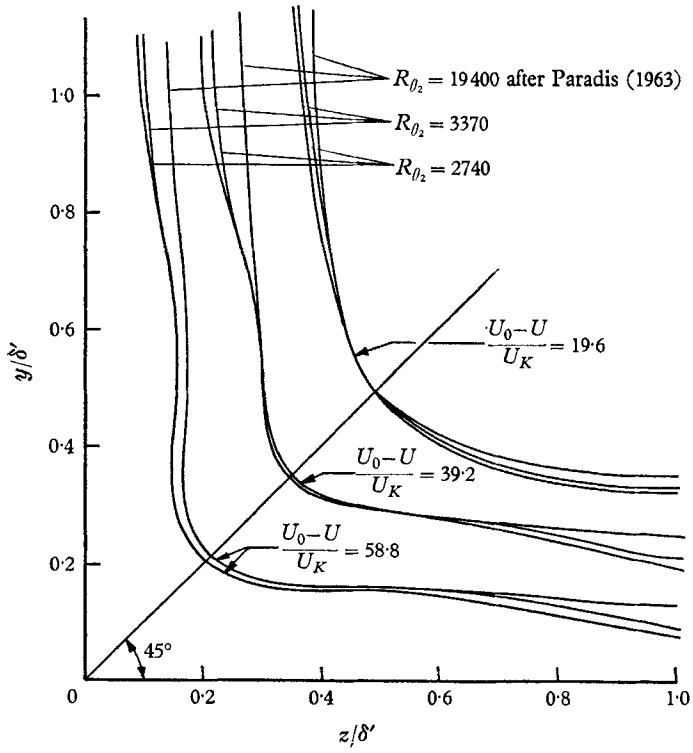

FIGURE 16. Velocities in the outer region from series I and Paradis (1963). Data points are omitted for clarity.

agreement was very poor for both these cases so that the correlation fails for adverse pressure gradients.

The correlation does not apply for low values of $U_K z/\nu$ and larger values of $U_K y/\nu$ or vice versa since in these regions the two-dimensional logarithmic law holds.

The results of Paradis (1963) away from the plane of symmetry but deep in the corner are not given so that checks using this data are not possible in this region.

In the region specified by the general form

$$(U_0 - U)/U_K = g_4(y/\delta', z/\delta')$$

it is possible to compare the present measurements for zero pressure gradient and those of Paradis by plotting lines of constant $(U_0 - U)/U_K$ against y/δ' and z/δ'. This is done in figure 16. Only the mean lines as obtained from the various data are given for clarity. The agreement is seen to be fairly good out to values of y/δ' and z/δ' of about 0·6. The failure of the correlation at this range is easily explained. Equation (12) depends for its validity on the assumption that U_{τ_2} has a negligible effect in the region compared to U_K. At large values of y/δ' or z/δ' this is obviously no longer true. The different dependence of U_{τ_2} and U_K upon Reynolds number would explain the difference in form of the lines of constant velocity in this region which are observed in figure 16.

It should be noted in closing this discussion that the various similarity arguments used to describe the x-direction flow in zero pressure gradient should also apply in their general form to the expected secondary currents in the various regions. Unfortunately reliable experimental measurements of secondary currents are not available so it is not possible to test this conclusion against experimental evidence.

7. Secondary currents

A streamwise vorticity equation containing small order terms is easily derived from the full Navier–Stokes equations by eliminating pressure from the equations. The result is similar to the equation studied by Brundrett & Baines (1964) in the fully developed square duct case. However, the appearance of additional terms which include derivatives of quantities with respect to x complicate the present flow. These terms will also produce vorticity of an unknown form and the analysis would be considerably more complicated than the square duct case. An experimental study would also present problems since terms of the type of $U(\partial V/\partial x)$ would need to be measured. In spite of the fairly obvious existence of these currents (see figures 3, 4 and 5 where the distortion of flow variables is quite similar to the case of fully developed square duct flow) their analysis would seem to be extremely difficult.

8. Conclusions

(i) A momentum integral equation closely analogous to that used in two-dimensional boundary layers is easily derived for the corner boundary layer.

The use of this equation is, however, limited by the difficulty of measuring the parameters which appear.

(ii) Similarity arguments similar to those used in two-dimensional boundary layers may be used to describe the turbulent flow in corners. More data at a wider range of Reynolds numbers is needed to justify these relations.

(iii) The experimental evidence suggests secondary currents in this type of flow but no analysis is available at present.

I am indebted to the Athlone Committee of the Board of Trade and to the National Research Council of Canada for their financial support of this work and to Professor W. A. Mair for his help and guidance.

REFERENCES

BRAGG, G. M. 1965 The turbulent boundary layer in a corner. Ph.D. Thesis, Engineering Department, University of Cambridge.

BRUNDRETT, E. & BAINES, W. D. 1964 The production and diffusion of vorticity in duct flow. *J. Fluid Mech.* **19**, 375.

DAVIES, E. B. & YOUNG, A. D. 1963 Streamwise edge effects in the turbulent boundary layer on a flat plate of finite aspect ratio. *Aero. Res. Counc. R. & M.* no. 3367.

EICHELBRENNER, E. A. 1961 La couche-limite turbulente à l'intérieur d'un dièdre. *La Recherche Aéronautique*, no. 83, 3.

EICHELBRENNER, E. A. 1965 Remarques sur la détermination de l'écoulement secondaire dans la couche-limite turbulente à l'intérieur d'un diedre. *La recherche Aérospatiale*, no. 104, 3.

GERSTEN, K. & MIYASHIRO, H. 1960. Ein Verfahren zur Berechnung der Reibungsschicht entlang einer rechtwinkligen Ecke für inkompressible Strömung. Bericht 60/35 Institut für Strömungsmechanik der Technischen Hochschule, Braunschweig.

GESSNER, E. B. & JONES, J. B. 1961 A preliminary study of turbulence characteristics of flow along a corner. *J. Bas. Engng.* p. 657.

LEUTHEUSSER, H. 1963 Turbulent flow in rectangular ducts. *Am. Soc. of Civil Eng. J. of the Hydraulics Division*, **89**, HY 3, 1.

LOUIS, J. F. 1968 Stall phenomena in axial flow compressors. Ph.D. Thesis, Cambridge University.

PARADIS, M. A. 1963 Couche-limite turbulente à l'intérieur d'un dièdre. Master's Thesis, L'Université Laval.

PEARSON, J. R. A. 1957 Homogeneous turbulence and laminar viscous flow. Ph.D. Thesis, Cambridge University.